



OPEN ACCESS

EDITED BY
Zhiyang Li,
Nanjing Drum Tower Hospital, China

REVIEWED BY
Fernando Soto,
Stanford University, United States
Xiangang Ding,
Nanjing University of Posts and
Telecommunications, China

*CORRESPONDENCE
Qiang Ding,
dingqiang@njmu.edu.cn
Changmin Yu,
iamcmyu@njtech.edu.cn
Jifu Wei,
weijifu@njmu.edu.cn

[†]These authors have contributed equally
to this work and share first authorship

SPECIALTY SECTION
This article was submitted to Biosensors
and Biomolecular Electronics,
a section of the journal
Frontiers in Bioengineering and
Biotechnology

RECEIVED 29 July 2022
ACCEPTED 15 August 2022
PUBLISHED 06 September 2022

CITATION
Wang C, Zhang D, Yang H, Shi L, Li L,
Yu C, Wei J and Ding Q (2022), A light-
activated magnetic bead strategy
utilized in spatio-temporal controllable
exosomes isolation.
Front. Bioeng. Biotechnol. 10:1006374.
doi: 10.3389/fbioe.2022.1006374

COPYRIGHT
© 2022 Wang, Zhang, Yang, Shi, Li, Yu,
Wei and Ding. This is an open-access
article distributed under the terms of the
[Creative Commons Attribution License
\(CC BY\)](https://creativecommons.org/licenses/by/4.0/). The use, distribution or
reproduction in other forums is
permitted, provided the original
author(s) and the copyright owner(s) are
credited and that the original
publication in this journal is cited, in
accordance with accepted academic
practice. No use, distribution or
reproduction is permitted which does
not comply with these terms.

A light-activated magnetic bead strategy utilized in spatio-temporal controllable exosomes isolation

Chenhan Wang^{1†}, Duoteng Zhang^{2†}, Haiyan Yang^{1†}, Liang Shi¹,
Lin Li², Changmin Yu^{2*}, Jifu Wei^{3*} and Qiang Ding^{1*}

¹Jiangsu Breast Disease Center, The First Affiliated Hospital with Nanjing Medical University, Nanjing, China, ²Key Laboratory of Flexible Electronics (KLOFE) and Institute of Advanced Materials (IAM), Nanjing Tech University (NanjingTech), Nanjing, China, ³Department of Pharmacy, Jiangsu Cancer Hospital and Jiangsu Institute of Cancer Research and The Affiliated Cancer Hospital of Nanjing Medical University, Nanjing, China

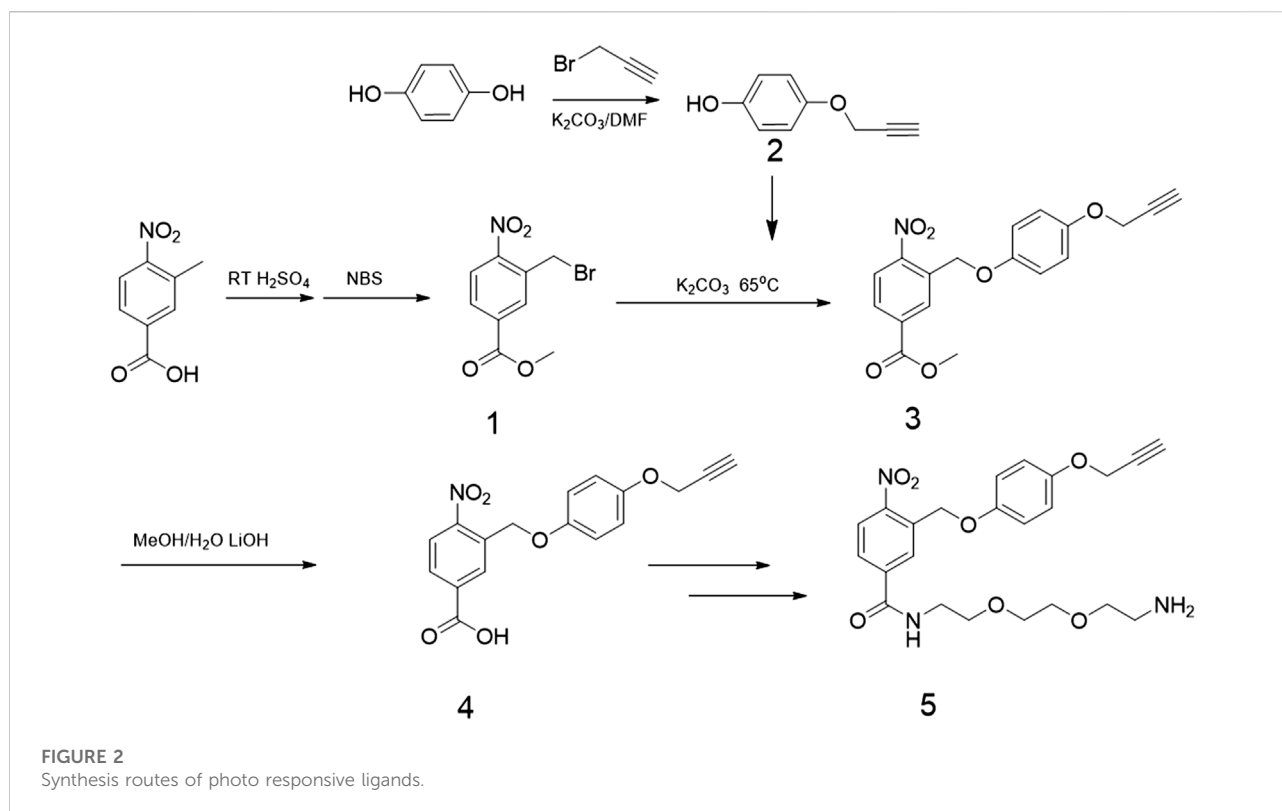
Tumor-derived exosomes are considered as a key biomarker in the field of liquid biopsy. However, conventional separation techniques such as ultracentrifugation, co-precipitation and column chromatography cannot isolate samples with high throughput, while traditional immunomagnetic separation techniques, due to steric effect of magnetic beads, reducing sensitivity of exosomes optical detection. Herein, we provide a novel and simple nanoplatfrom for spatiotemporally controlling extraction and elution of exosomes *via* magnetic separation and light-activated cargo release. In this system, magnetic beads are co-modified by photoresponsive groups -nitrobenzyl group and aptamers that are compatible with CD63—a highly expressed exosomal surface-specific protein. Through exosomes extracted from cell model and nude mice xenograft tumor model morphological characterization and proteomic analysis, results showed that our novel magnetic bead system outperformed current ultracentrifugation in serum exosome extraction in terms of extraction time, yield, and proportion of populations with high CD63 expression. This strategy may be a powerful tool for exosome isolation in clinical liquid biopsies of cancer disease.

KEYWORDS

exosome, cancer, magnetic separation, light-activated release, liquid biopsy

Introduction

Liquid biopsy is an emerging adjunctive detection method, which uses biological information carried by body fluid components such as blood, urine, sweat, et al. (Willms et al., 2018; Wang C et al., 2020; Descamps et al., 2022; Markou et al., 2022). Exosomes, a type of small extracellular vesicles with a size of 30–150 nm, are well-documented to participate in tumor development, e.g., stimulating the growth of tumor cells, suppressing anti-tumor immunity, promoting tumor cell migration and metastasis, et al. (Liu et al., 2018; Hofmann et al., 2020; Liao and Li, 2020; Chen et al., 2022; He et al., 2022). They are



Materials and methods

Materials and reagents

Magnetic beads (CSMN Beads-100, MBs, 100 nm) were purchased from So-Fe Biomedicine (Shanghai, China). The rest of chemical reagents used in the synthesis of nanodevices were purchased from Sinopharm Chemical Reagent Co. (Shanghai, China) and Sigma (Shanghai, China). SUM-1315 cells line was purchased from the Chinese Academy of Sciences (Shanghai, China). DMEM medium (11965092), Penicillin/streptomycin (15140122), and FBS (10099141C) were purchased from GIBCO (Shanghai, China). Anti-CD9 (13,403) primary antibodies were purchased from Cell Signaling Technology (Shanghai, China). Anti-CD63 (ab22595) and anti-calnexin (ab134045) primary antibodies were purchased from Abcam (Shanghai, China). Antirabbit HRP secondary antibodies (a0208), Enhanced-chemiluminescence (ECL) kits (P0018FS), and BCA kit (P0012S) were purchased from Beyotime. Biotechnology (Shanghai, China). CD63 aptamer with azide group was synthesized by Sangon (Shanghai, China), with the following sequence: 5'-CAC CCC ACC TCG CTC CCG TGA CAC TAA TGC TA-3'-N₃ (Zhang Z et al., 2019).

Synthesis of magnetic bead system (MBs-Apt₆₃)

Magnetic nanoparticle solution (600 μ l, 5 mg/ml) was added to a 1.5 ml centrifuge tube. The nanoparticles were precipitated to bottom of the centrifuge tube with magnets, and supernatant was removed. After being washed with water three times, the nanoparticles were redispersed in 3 ml of 2-morpholinoethanesulfonic acid (MES) buffer with ultrasound. 1-(3-Dimethylaminopropyl)-3-ethylcarbodiimide hydrochloride (EDC) (dissolved with MES, 2.5 mg/ml, 2 ml) and N-hydroxy succinimide (NHS) (dissolved with MES, 5 mg/ml, 1 ml) were then added, followed by sonication for 15 s. The centrifuge tube was sealed by sealing film and shaken at 37°C for 45 min. After that, the nanoparticles were deposited to the bottom of the centrifuge tube and washed twice with phosphate buffered saline (PBS) buffer. The nanoparticles were redispersed in 6 ml PBS. Compound 5 (the compound codes mentioned in this paper were shown in Figure 2) in dimethyl sulfoxide (DMSO) (60 μ l, 100 mg/ml) was added to the centrifuge tube and mixed by ultrasound. The mixture was oscillated at 37°C for 12 h. After removal of the supernatant, the CD63 aptamer with azide group was added into the nanoparticles' aqueous solution at a 1:1 M ratio. 1 mol% copper sulfate pentahydrate and 5 mol% sodium ascorbates were added and

solution was shaken at room temperature for 8 h to get the final magnetic bead system (MBS-Apt₆₃).

Cell culture

SUM-1315 cells tested negative for *mycoplasma* were cultured in DMEM supplemented with 10% FBS and 1% penicillin–streptomycin. All cells were cultured in an incubator under 5% CO₂ at 37°C.

Agarose gel electrophoresis

The aptamer-MBs mixture system was loaded into each well of the agarose gel and separated *via* electrophoresis. Target oligonucleotides were detected with Gel-Red kits.

Isolation of exosomes by UC from cell supernatant and serum

Exosomes were extracted from the supernatant of SUM-1315 cells or serum in the following steps: centrifugation was performed at 4°C at 2,000 × *g* for 10 min, and the supernatant was kept and centrifuged at 10,000 × *g* for another 30 min to further remove the debris. These samples were transferred to UC tubes and centrifuged at 110,000 × *g* for 75 min, followed by removal of the supernatant. The precipitates were resuspended and diluted with 1×PBS, and filtered through 0.22 μm membrane. The product was centrifugated again at 110,000 × *g* for 75 min, and the supernatant was discarded. The pellets were resuspended with 1×PBS and stored at –80°C for further use.

Isolation of exosomes by MBs -Apt₆₃

Magnetic beads (0.1 μg) were added to every 500 μl of exosome suspension or serum to capture exosomes. The binding process was carried out on a shaker. After 20 min, the EP tube was put in a tube rack with a permanent magnet placed against the tube bottom. The supernatant was discarded. After 5 min of precipitation, and the pellets were resuspended in PBS and placed under UV light for 20 min. After elution of the exosomes, the bare magnetic beads were removed by permanent magnets after of 5 min's adsorption time, and the exosome-containing supernatant was retained in 500 μl PBS.

Transmission electron microscope (TEM)

PBS solution (20 μl) containing exosomes was added to a carbon-coated copper grid and adsorbed. After cleaning with

PBS, the copper grid was fixed in 1% glutaraldehyde for 2 min. The excess solution was removed by using paper towel to blot the edges of each grid. Then the sample was negatively stained with saturated uranyl acetate solution and incubated at room temperature for 1min. The unevaporated solution is removed with paper towel. The samples were observed under a transmission electron microscope.

Nanoparticle tracking analysis (NTA)

Nanoparticle tracking analysis was performed on ZetaVIEW S/N 17-310 and all NTA measurements were performed using the same setup to ensure consistent results. The exosomes were diluted in PBS to obtain 50 particles in each field of vision for optimal counting.

Dynamic light scattering (DLS)

Dynamic light scattering (DLS) measurements were conducted on a Nano ZS instrument (Malvern, United Kingdom). All samples were resuspended in PBS, and measured with the same instrument setup.

Western blotting

Exosome suspension (10 μl) was loaded into SDS-PAGE and then separated by electrophoresis. Proteins were transferred onto polyvinylidene fluoride membranes and blocked with 5% skim milk. The primary anti-CD63 and anti-CD9 antibodies were used, followed by incubation with HRP-conjugated secondary antibodies. Target proteins were detected with enhanced-ECL kits.

Animal models

BALB/C-nude mice (female, 4 weeks) were purchased from Model Animal Research Center, Nanjing University. The animal experiment was approved by the Ethics Committee of Nanjing Medical University. We confirmed that all animal experiments are complied with National Institutes of Health guide for the care and use of Laboratory animals (NIH Publications No. 8023, revised 1978). The animals were raised at 25°C with 60% humidity. 2 × 10⁶ of sum-1315 cells were inoculated into the back of each nude mouse. 10 days later, blood was collected from the posterior venous cluster of the eyeball. The blood was placed at room temperature for 2 h and centrifuged at 3000 rpm for 10 min at 4°C, and the upper serum was preserved. The serum of nude mice was stored at –80°C.

High sensitivity flow cytometry

Exosomes were incubated with 20 μ l fluorescently labeled antibody (CD63) at 37°C for 30 min in dark. Then 1 ml of pre-cooled PBS (4°C) was added, followed by centrifugation at 110,000 g for 70 min. The supernatant was carefully removed and 1 ml of pre-cooled PBS (4°C) was added to resuspend. The solution was then centrifuged at 110,000 g at 4°C for 70 min, and the supernatant was carefully removed, followed by resuspension of pellets in 50 μ l of precooled PBS (4°C) for analysis.

Proteomic analysis of exosomes

Exosome suspension was treated with 7 M urea, 2%SDS, and 1 \times Protease Inhibitor Cocktail. Protein concentration was determined using the BCA protein detection kit, and then the sample was processed with nuclease digestion, reduction/alkylation, acetone precipitation, and lysine-C/trypsin digestion. Desalination was carried out in the monospin column using 0.1% trifluoroacetic acid (TFA) and acetonitrile. After vacuum drying, 0.1%FA was added to redissolve the sample, and a 1–2 μ g of sample was analyzed. The separation was performed with Easy-NLC 1000 (Thermo Scientific, United States) using an analytical column (C18, 1.9 μ m, 75 μ m \times 20 cm) at a flow rate of 300 NL/min. Orbitrap Fusion Lumos (Thermo Scientific, United States) was used as a mass spectrometer. Data Dependent Acquisition (DDA) model was used for tandem mass spectrometry. The full-scan resolution was 60,000 (FWHM), the mass-charge ratio range was set to M/Z 350–1800, and the impact energy was set to 30% in HCD fragmentation mode. The original mass spectrometry data were collected and analyzed using the mass informatics platform Proteome Discoverer 2.4 (Thermo Fisher).

Statistics

Origin 2019 and GraphPad Prism 8.0 were used for statistical calculation of all histograms, and one-way anova was used for calculation of mean and variance.

Results

Synthesis of UV-responsive magnetic bead system (MBs-Apt₆₃)

The 2-nitrobenzyl groups were used as photo-cleavable linkers to anchor CD63 aptamers onto MBs. The detailed synthesis route is shown in Figure 2, and the chemical synthesis steps of photoresponsive ligands are described in

Supplementary Material S1. The structure of MBs-Apt₆₃ is shown in Figure 1. Firstly, the photo-cleavable linkers were anchored onto the surface of MBs *via* a moderate amination reaction. To selectively capture exosomes, CD63 aptamers were finally conjugated with the MBs through click reaction. The final UV-responsive magnetic bead system (MBs-Apt₆₃) was characterized for Zeta potential, infrared spectroscopy, and dynamic light scattering (DLS) size (Supplementary Figure S2 and Supplementary Figure S10).

Magnetic beads respond to UV *in vitro*

We measured the UV responsiveness of the magnetic beads with a concentration at the range of 0–10 μ g/ml, while the time of exposure to UV light was between 0 and 30 min. In Figures 3A,B, it was found that within the range of 0–10 μ g/ml, the light-responsive groups of magnetic beads were highly sensitive to and effectively cleaved by UV light. The CD63 aptamers were rapidly released from MBs-Apt₆₃ under irradiation, which also showed obvious time dependence. With increased exposure time, the amount of released free aptamers increased, and reached the maximum after 15 min of UV exposure.

Preparation and validation of exosomes

To test the ability of MBs-Apt₆₃ to capture exosomes, we firstly extracted tumor exosomes from the cultural medium of breast cancer cell line SUM-1315 by UC. Western blotting analysis of exosomes showed the presence of CD9, CD63 (two common surface markers of exosomes) and calnexin (endoplasmic reticulum protein), indicating the successful preparation (Figure 3C). In DLS analysis, the exosomes showed an average size of 56 nm (Figure 3D), in line with characteristic particle size of exosomes (30–150 nm). Finally, we used TEM to observe the morphology of exosomes (Figures 3E,F), which displayed a typical lipid bilayer structure and a size in the range of 50–100 nm.

Capturing exosomes with MBs-Apt₆₃ and elution with UV light

The process of isolating exosomes from cell supernatant or serum is shown in Figure 4A, which involves beads binding and exosome elution. DLS analysis was performed after MBs binding to exosomes and UV-triggered elution, which showed a size of 250 and 190 nm, respectively. (Figures 4B,C). In Figure 4C, the magnetic bead components were not removed in the system after ultraviolet dissociation. This reduced shift in maximum peak particle size from 256 to 190 nm indicated

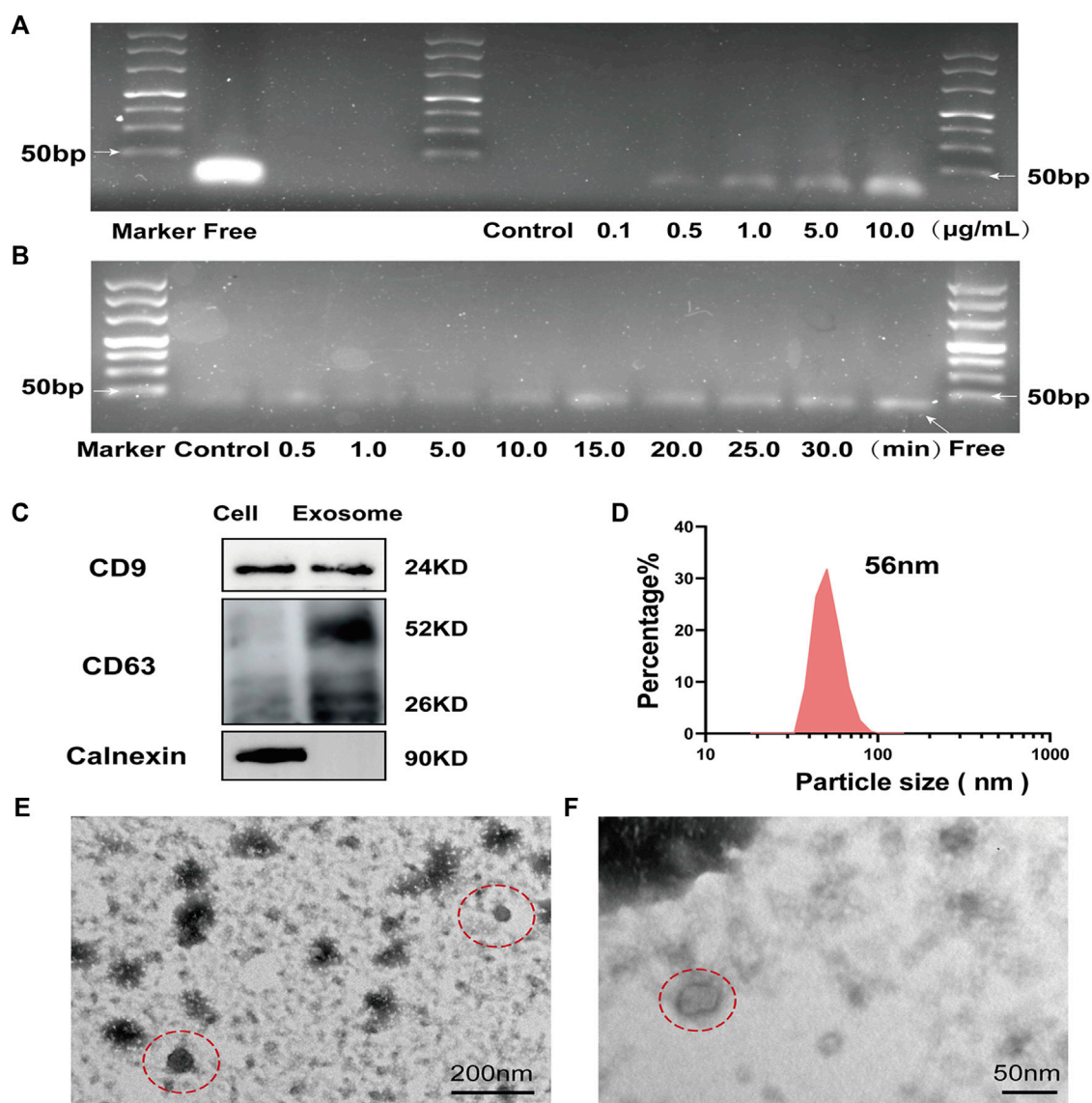


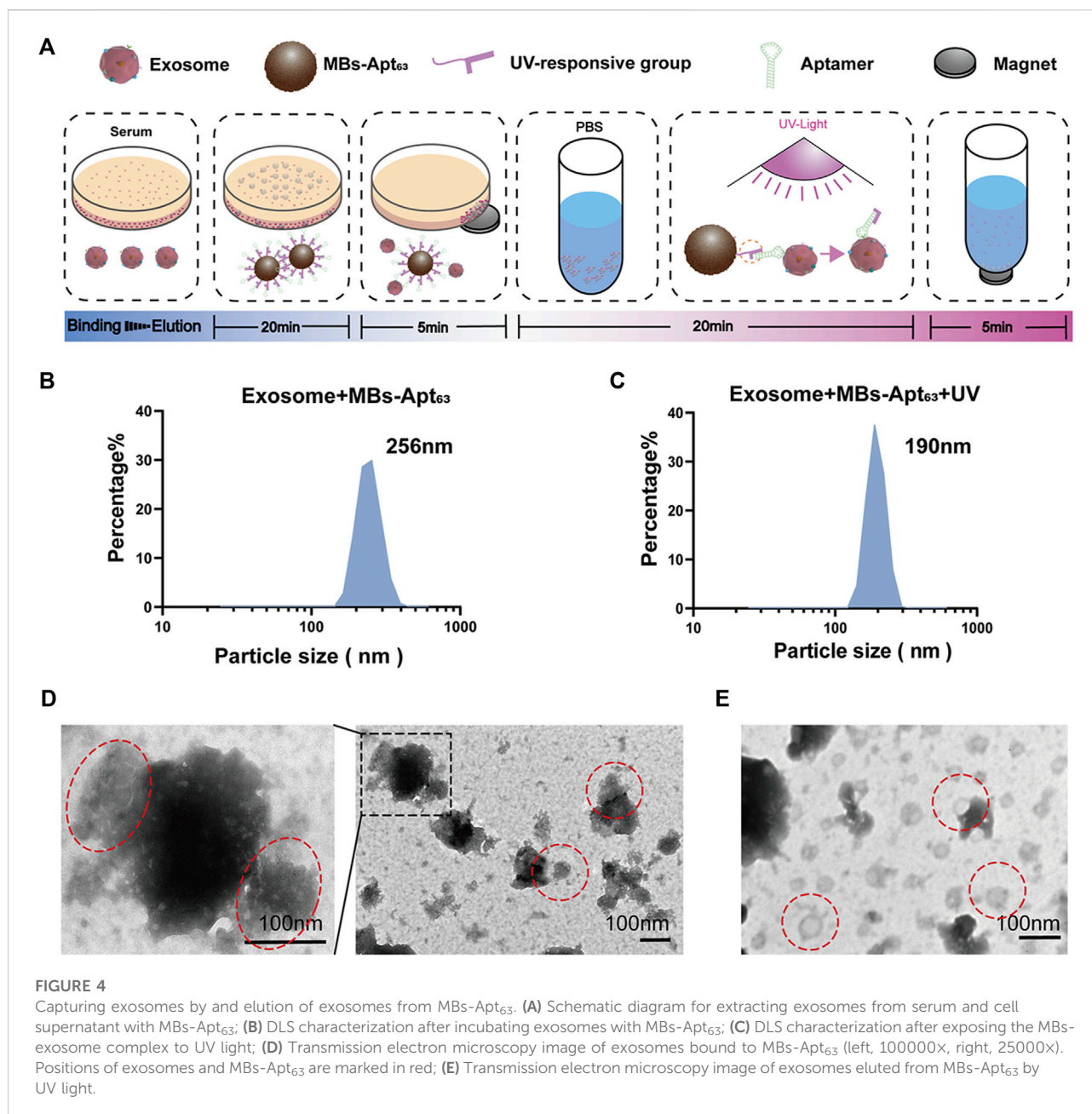
FIGURE 3

Response of MBs-Apt₆₃ to UV *in vitro* and identification of exosomes (A) Agarose gel electrophoresis (molecular weight of free aptamer = 32 bp) of MBs-Apt₆₃ at different concentrations after UV exposure; (B) Agarose gel electrophoresis of MBs-Apt₆₃ (10.0 µg/ml) after exposure to UV for different times (molecular weight of free aptamer = 32 bp). (C) The expression of CD9, CD63 and calnexin determined by western blotting; (D) The particle size of breast cancer cell exosomes characterized by DLS; (E, F) Transmission electron microscopy image of breast cancer exosomes (magnification = 50000x in C and 100000x in D, exosomes are shown in the red dotted circle).

the elution of exosomes from the MBs after UV exposure. To further elaborate the binding and elution processes, TEM was used to observe the MBs-exosome complex before and after UV-triggered cargo release. Typical MBs bound to many exosomes were clearly seen before exposure to UV light (Figure 4D), whereas only purified exosomes could be observed after UV-induced release of exosomes and removal of magnetic beads by permanent magnets (Figure 4E).

Application of MBs-Apt₆₃ in the separation of serum exosomes from breast cancer

To evaluating the performance of this novel MBs system in isolating serum exosomes, we established mice models of triple-negative breast cancer using human breast cancer SUM-1315 cells. We collected the serum when the tumor grew to about 800 mm³, and then isolated exosomes with MBs-Apt₆₃ and conventional UC respectively. We firstly analyzed the particle



size distribution (Figure 5A) and particle concentration of exosomes (Figure 5B) with NTA. Results showed that the particle size distribution of exosomes isolated by MBs-Apt₆₃ and UC was similarly uniform, both of which were about 100 nm. While the serum concentration of exosomes acquired by UC is lower compared with that by MBs-Apt₆₃ (2.5×10^9 /ml versus 4.0×10^9 /ml) according to the particle count analysis, indicating higher efficiency of MBs-Apt₆₃ in extracting serum exosomes.

Next, we used the high sensitivity flow cytometry (HSFC) system to analyze the expression of CD63 on exosomes separated

by UC and MBs-Apt₆₃ (Figure 5C). The results showed that the expression abundance of CD63 was 4.9% in exosomes extracted by MBs-Apt₆₃, which is much higher (0.4%) in exosomes separated by UC method. Therefore, the light strategy in MBs-Apt₆₃ system improved the purity of exosomes with high expression of CD63.

In exosome-based liquid biopsies, diagnostic value ultimately comes from biomarkers in exosomes. In this study, proteins in exosomes separated by UC and magnetic beads were both analyzed by liquid mass spectrometry. We conducted a database search and comparison according to Proteome

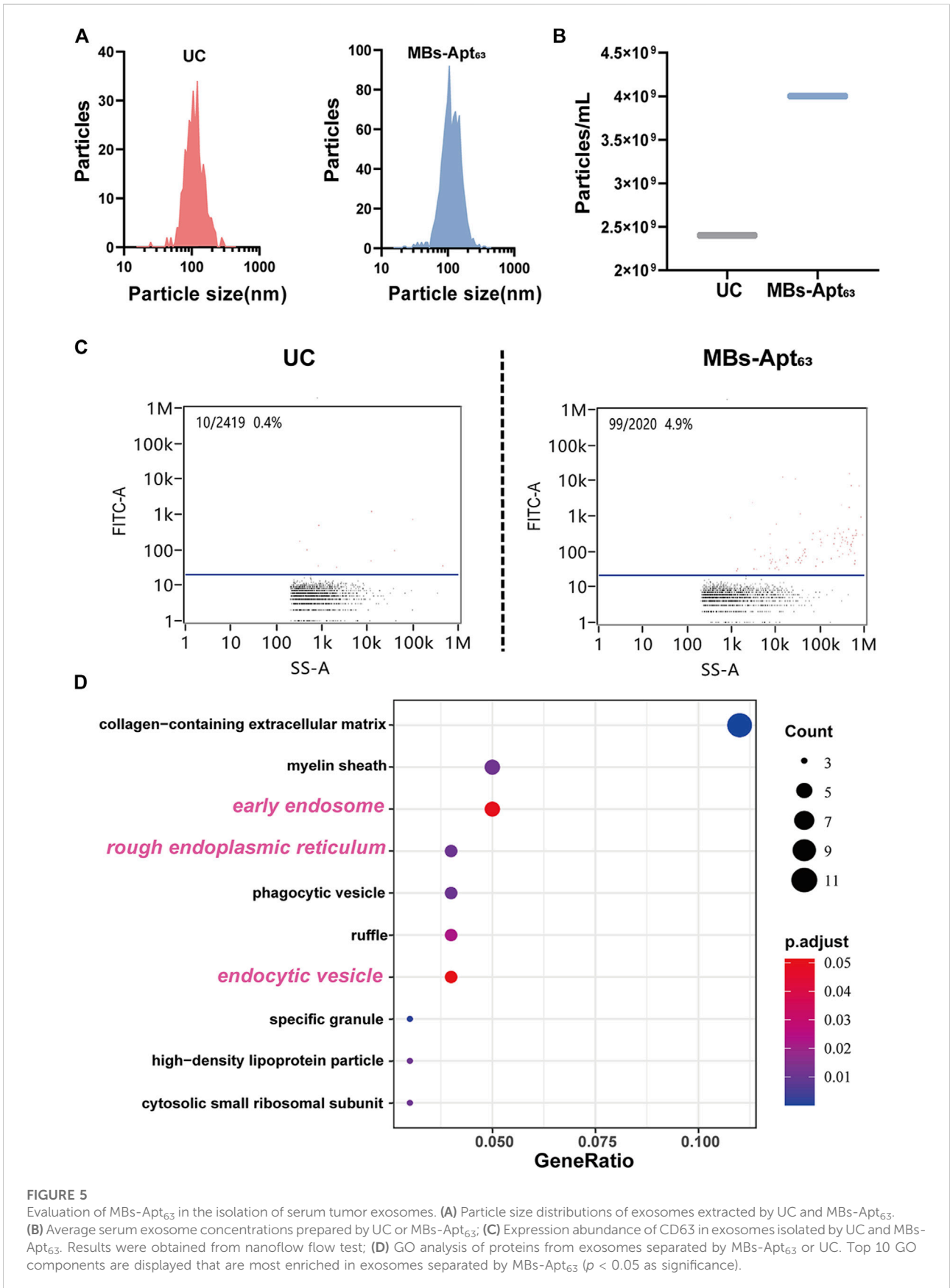


FIGURE 5

Evaluation of MBs-Apt₆₃ in the isolation of serum tumor exosomes. (A) Particle size distributions of exosomes extracted by UC and MBs-Apt₆₃. (B) Average serum exosome concentrations prepared by UC or MBs-Apt₆₃; (C) Expression abundance of CD63 in exosomes isolated by UC and MBs-Apt₆₃. Results were obtained from nanoflow flow test; (D) GO analysis of proteins from exosomes separated by MBs-Apt₆₃ or UC. Top 10 GO components are displayed that are most enriched in exosomes separated by MBs-Apt₆₃ ($p < 0.05$ as significance).

Discoverer 2.4 system. Specific database search parameters are shown in [Supplementary Table S2](#). The relevant quality control information is shown in [Supplementary Figure S5](#). 1044 proteins were identified in the exosomes isolated by UC, while only 677 proteins were detected in the exosomes separated by magnetic beads ([Supplementary Table S3](#)). To verify that our optically controlled MBs-Apt₆₃ preserved more exosome-related proteins, we performed GO analysis on high-expression set of exosome proteins extracted by MBs-Apt₆₃ versus UC. The screening criteria for differential proteins between the two groups were:

(1), Inter-group ratio ≥ 4 (2), Unique Peptides ≥ 2 .

Among the top 10 GO components that were significantly higher in exosomes extracted by MBs-Apt₆₃, three are related to exosome formation, including rough endoplasmic reticulum, early endosomes, and endocytic vesicles ([Figure 5D](#)), indicating a higher expression abundance of exosome-related proteins in CD63 positive exosomes separated by MBs-Apt₆₃.

Discussions

In this study, we developed a facile light-responsive magnetic bead sorting system for extracting exosomes from breast cancer. In our strategy, 2-nitrobenzene is designed as the surface ligand of the magnetic beads, whose UV responsiveness allows for spatiotemporal control of exosome separation with minimum interference with serum composition. From a practical perspective, it requires less time and smaller sample volume, and does not need sophisticated instruments. More importantly, this system can largely improve the efficiency of exosome isolation, maximizing the purity and integrity of the exosomes. At the same time, without the interference of magnetic beads, exosomes in the real liquid environment can greatly improve the efficiency of the labeled enzyme and substrate reaction. In addition, the masking effect of magnetic beads themselves will be eliminated. Therefore, this method should be able to improve the sensitivity of subsequent detection.

Previous studies have reported considerable progress in the field of liquid biopsy, particularly some nanomaterial-based liquid biopsy techniques ([Zhang P et al., 2019](#); [Tian et al., 2019](#); [Huang et al., 2020](#); [Xia et al., 2020](#); [Chen et al., 2021](#); [He et al., 2021](#)). On this basis, some studies have significantly improved the sensitivity of liquid biopsies, while others have looked at reducing the amount of fluid used in this process ([Huang et al., 2019](#); [Li et al., 2019](#); [Kim et al., 2020](#); [Jiang et al., 2021](#)). In this study, the operation mode and sample requirements of liquid biopsy were further simplified. Firstly, the extraction method of exosomes by illumination and magnetic separation does not require additional reagents and processing time, which ensures reproducibility of extraction procedures, making our magnetic bead system can be used in large quantities

in clinical practice. Secondly, the spatiotemporally controllable extraction method provides a simple exosome release strategy to remove the steric effect based on magnetic bead fixation, so that magnetic bead-based exosome detection can achieve better detection efficiency in the liquid phase reaction system. At the same time, as most research on UV response devices, the wavelength of UV light used in this study is about 254 nm. It has been shown in some studies that there is no relevant evidence to confirm that 254 nm ultraviolet light will cause damage to proteins under certain conditions of time and intensity ([O'Brien et al., 2014](#); [Cannon et al., 2014](#)).

Our experimental results basically demonstrate the clinical application prospect of the system. Compared with traditional ultracentrifugation, the number of exosomes extracted from serum by our system increased by 60%. At the same time, the purity of proteins represented by CD63 was increased by 10 times. Through proteomic analysis, we also confirmed that the MBs-Apt₆₃ preserved more protein components from exosomes. It indicated that, compared with traditional exosome extraction methods in the field of liquid biopsy for clinical cancer patients, this system can obtain the information of tumor in patients' serum in a relatively comprehensive way, thus providing more reference value for implementation of diagnosis and treatment process. In the future, by changing the aptamers, our strategy provides a flexible approach to pathological analysis of breast cancer for personalized medicine, and its large-scale application can also supply a new platform for broadening the application scope of liquid biopsy of cancer. At the same time, this light-activated magnetic bead strategy also establishes the possibility to nondestructively enrich specific functional cell exosomes for cancer disease treatment ([Fang et al., 2022](#)).

Data availability statement

The original contributions presented in the study are included in the article/[Supplementary Material](#); further inquiries can be directed to the corresponding authors.

Ethics statement

The animal study was reviewed and approved by Ethics Committee of Nanjing Medical University.

Author contributions

QD and CY conceived the idea and supervised the research; CW and DZ designed the experiments; CW, DZ, and HY carried out specific experimental operations; CW, DZ, QD, JW, LL, and CY co-wrote the paper; LS provides clinical consulting and data

analysis; All authors discussed the results and commented on the manuscript.

Funding

This study was supported by the National Natural Science Foundation of China (81972486).

Conflict of interest

The authors declare that the research was conducted in the absence of any commercial or financial relationships that could be construed as a potential conflict of interest.

References

- Cannon, J. R., Cammarata, M. B., Robotham, S. A., Cotham, V. C., Shaw, J. B., Fellers, R. T., et al. (2014). Ultraviolet photodissociation for characterization of whole proteins on a chromatographic time scale. *Anal. Chem.* 86, 2185–2192. doi:10.1021/ac403859a
- Chang, D. J., Yoon, E. Y., Lee, G. B., Kim, S. O., Kim, W. J., Kim, Y. M., et al. (2009). Design, synthesis and identification of novel colchicine-derived immunosuppressant. *Bioorg. Med. Chem. Lett.* 19, 4416–4420. doi:10.1016/j.bmcl.2009.05.054
- Chen, W., Li, Z., Cheng, W., Wu, T., Li, J., Li, X., et al. (2021). Surface plasmon resonance biosensor for exosome detection based on reformatory tyramine signal amplification activated by molecular aptamer beacon. *J. Nanobiotechnology* 19, 450. doi:10.1186/s12951-021-01210-x
- Chen, W., Zhang, Y., Di, K., Liu, C., Xia, Y., Ding, S., et al. (2022). A washing-free and easy-to-operate fluorescent biosensor for highly efficient detection of breast cancer-derived exosomes. *Front. Bioeng. Biotechnol.* 10, 945858. doi:10.3389/fbioe.2022.945858
- Choi, D. Y., Park, J. N., Paek, S. H., and Choi, S. C. (2022). Detecting early-stage malignant melanoma using a calcium switch-enriched exosome subpopulation containing tumor markers as a sample. *Biosens. Bioelectron.* X. 198, 113828. doi:10.1016/j.bios.2021.113828
- Descamps, L., Le Roy, D., and Deman, A. L. (2022). Microfluidic-based technologies for CTC isolation: a review of 10 years of intense efforts towards liquid biopsy. *Int. J. Mol. Sci.* 23, 1981. doi:10.3390/ijms23041981
- Fang, Z. W., Zhang, X. Y., Wu, J., and Huang, H. (2022). Exosome based miRNA delivery strategy for disease treatment. *Chin. Chem. Lett.* 33, 1693–1704. doi:10.1016/j.ccl.2021.11.050
- Gao, F., Jiao, F., Xia, C., Zhao, Y., Ying, W., Xie, Y., et al. (2019). A novel strategy for facile serum exosome isolation based on specific interactions between phospholipid bilayers and TiO₂. *Chem. Sci.* 10, 1579–1588. doi:10.1039/c8sc04197k
- Guo, S., Xu, J., Estell, A. P., Ivory, C. F., Du, D., Lin, Y., et al. (2020). Paper-based ITP technology: An application to specific cancer-derived exosome detection and analysis. *Biosens. Bioelectron.* X. 164, 112292. doi:10.1016/j.bios.2020.112292
- Gurunathan, S., Kang, M. H., Jeyaraj, M., Qasim, M., and Kim, J. H. (2019). Review of the isolation, characterization, biological function, and multifarious therapeutic approaches of exosomes. *Cells* 8, 307. doi:10.3390/cells8040307
- He, L., Huang, R., Xiao, P., Liu, Y., Jin, L., Liu, H., et al. (2021). Current signal amplification strategies in aptamer-based electrochemical biosensor: A review. *Chin. Chem. Lett.* 32, 1593–1602. doi:10.1016/j.ccl.2020.12.054
- He, L., Yu, X., Huang, R., Jin, L., Liu, Y., Deng, Y., et al. (2022). A novel specific and ultrasensitive method detecting extracellular vesicles secreted from lung cancer by padlock probe-based exponential rolling circle amplification. *Nano Today* 22, 101334. doi:10.1016/j.nantod.2021.101334
- Hentzen, N. B., Mogaki, R., Otake, S., Okuro, K., and Aida, T. (2020). Intracellular photoactivation of caspase-3 by molecular glues for spatiotemporal apoptosis induction. *J. Am. Chem. Soc.* 142, 8080–8084. doi:10.1021/jacs.0c01823

Publisher's note

All claims expressed in this article are solely those of the authors and do not necessarily represent those of their affiliated organizations, or those of the publisher, the editors and the reviewers. Any product that may be evaluated in this article, or claim that may be made by its manufacturer, is not guaranteed or endorsed by the publisher.

Supplementary material

The Supplementary Material for this article can be found online at: <https://www.frontiersin.org/articles/10.3389/fbioe.2022.1006374/full#supplementary-material>

- Hofmann, L., Ludwig, S., Vahl, J. M., Brunner, C., Hoffmann, T. K., and Theodoraki, M. N. (2020). The emerging role of exosomes in diagnosis, prognosis, and therapy in head and neck cancer. *Int. J. Mol. Sci.* 21, 4072. doi:10.3390/ijms21114072
- Huang, R., He, L., Xia, Y., Xu, H., Liu, C., Xie, H., et al. (2019). A sensitive aptasensor based on a Hemin/G-Quadruplex-assisted signal amplification strategy for electrochemical detection of gastric cancer exosomes. *Small* 15, e1900735. doi:10.1002/smll.201900735
- Huang, R., He, L., Li, S., Liu, H., Jin, L., Chen, Z., et al. (2020). A simple fluorescence aptasensor for gastric cancer exosome detection based on branched rolling circle amplification. *Nanoscale* 12, 2445–2451. doi:10.1039/c9nr08747h
- Ibsen, S. D., Wright, J., Lewis, J. M., Kim, S., Ko, S. Y., Ong, J., et al. (2017). Rapid isolation and detection of exosomes and associated biomarkers from plasma. *ACS Nano* 11, 6641–6651. doi:10.1021/acsnano.7b00549
- Jiang, K. M., Wu, Y. A., Li, Z. H., Chen, J., Shi, M., and Meng, H. (2021). Molecular recognition triggered aptamer cascade for ultrasensitive detection of exosomes in clinical serum samples. *Chin. Chem. Lett.* 32, 1827–1830. doi:10.1016/j.ccl.2020.11.031
- Kim, Y. B., Yang, J. S., Lee, G. B., and Moon, M. H. (2020). Evaluation of exosome separation from human serum by frit-inlet asymmetrical flow field-flow fractionation and multiangle light scattering. *Anal. Chim. Acta* X. 1124, 137–145. doi:10.1016/j.aca.2020.05.031
- Kobayashi, T., Komatsu, T., Kamiya, M., Campos, C., Gonzalez-Gaitan, M., Terai, T., et al. (2012). Highly activatable and environment-insensitive optical highlighters for selective spatiotemporal imaging of target proteins. *J. Am. Chem. Soc.* 134, 11153–11160. doi:10.1021/ja212125w
- Lai, J., Yu, A., Yang, L., Zhang, Y., Shah, B. P., and Lee, K. B. (2016). Development of photoactivated fluorescent N-hydroxyoxindoles and their application for cell-selective imaging. *Chem. Eur. J.* 22, 6361–6367. doi:10.1002/chem.201600547
- Li, Z., Hu, C., Jia, J., Xia, Y., Xie, H., Shen, M., et al. (2019). Establishment and evaluation of a simple size-selective method for exosome enrichment and purification. *J. Biomed. Nanotechnol.* 15, 1090–1096. doi:10.1166/jbn.2019.2768
- Liao, H., and Li, H. (2020). Advances in the detection technologies and clinical applications of circulating tumor DNA in metastatic breast cancer. *Cancer Manag. Res.* 12, 3547–3560. doi:10.2147/cmar.s249041
- Liu, C., Xu, X., Li, B., Situ, B., Pan, W., Hu, Y., et al. (2018). Single-exosome-counting immunoassays for cancer diagnostics. *Nano Lett.* 18, 4226–4232. doi:10.1021/acs.nanolett.8b01184
- Lu, Y. X., Tong, Z. D., Mao, H. J., Jian, X., Zhou, L., Qiu, S., et al. (2022). Multiple exosome RNA analysis methods for lung cancer diagnosis through integrated on-chip microfluidic system. *Chin. Chem. Lett.* 33, 3188–3192. doi:10.1016/j.ccl.2021.12.045
- Markou, A., Tzanikou, E., and Lianidou, E. (2022). The potential of liquid biopsy in the management of cancer patients. *Semin. Cancer Biol.* 22, 00069–00079. doi:10.1016/j.semcancer.2022.03.013

- Mathieu, M., Névo, N., Jouve, M., Valenzuela, J. I., Maurin, M., Verweij, F. J., et al. (2021). Specificities of exosome versus small ectosome secretion revealed by live intracellular tracking of CD63 and CD9. *Nat. Commun.* 12, 4389–4407. doi:10.1038/s41467-021-24384-2
- Momen-Heravi, F., Balaj, L., Alian, S., Mantel, P. Y., Halleck, A. E., Trachtenberg, A. J., et al. (2013). Current methods for the isolation of extracellular vesicles. *Biol. Chem.* 394, 1253–1262. doi:10.1515/hsz-2013-0141
- O'Brien, J. P., Li, W., Zhang, Y., and Brodbelt, J. S. (2014). Characterization of native protein complexes using ultraviolet photodissociation mass spectrometry. *J. Am. Chem. Soc.* 136, 12920–12928. doi:10.1021/ja505217w
- Puhka, M., Thierens, L., Nicorici, D., Forsman, T., Mirtti, T., af Hallstrom, T., et al. (2022). Exploration of extracellular vesicle miRNAs, targeted mRNAs and pathways in prostate cancer: Relation to disease status and progression. *Cancers (Basel)*. 14, 532. doi:10.3390/cancers14030532
- Shen, M., Di, K., He, H., Xia, Y., Xie, H., Huang, R., et al. (2020). Progress in exosome associated tumor markers and their detection methods. *Mol. Biomed.* 1, 3. doi:10.1186/s43556-020-00002-3
- Song, Z., Mao, J., Barrero, R. A., Wang, P., Zhang, F., and Wang, T. (2020). Development of a CD63 aptamer for efficient cancer immunochemistry and immunoaffinity-based exosome isolation. *Molecules* 25, 5585–5601. doi:10.3390/molecules25235585
- Sung, B. H., von Lersner, A., Guerrero, J., Krystofiak, E. S., Inman, D., Pelletier, R., et al. (2020). A live cell reporter of exosome secretion and uptake reveals pathfinding behavior of migrating cells. *Nat. Commun.* 11, 2092. doi:10.1038/s41467-020-15747-2
- Tian, X., Shen, H., Li, Z., Wang, T., and Wang, S. (2019). Tumor-derived exosomes, myeloid-derived suppressor cells, and tumor microenvironment. *J. Hematol. Oncol.* 12, 84. doi:10.1186/s13045-019-0772-z
- Wang, L., Chen, B., Peng, P., Hu, W., Liu, Z., Pei, X., et al. (2017). Fluorescence imaging mitochondrial copper(II) via photocontrollable fluorogenic probe in live cells. *Chin. Chem. Lett.* 28, 1965–1968. doi:10.1016/j.ccl.2017.07.016
- Wang, C., Senapati, S., and Chang, H. C. (2020). Liquid biopsy technologies based on membrane microfluidics: High-yield purification and selective quantification of biomarkers in nanocarriers. *Electrophoresis* 41, 1878–1892. doi:10.1002/elps.202000015
- Wang, S., Khan, A., Huang, R., Ye, S., Di, K., Xiong, T., et al. (2020). Recent advances in single extracellular vesicle detection methods. *Biosens. Bioelectron.* X, 154, 112056. doi:10.1016/j.bios.2020.112056
- Willms, E., Cabanas, C., Mager, I., Wood, M. J. A., and Vader, P. (2018). Extracellular vesicle heterogeneity: Subpopulations, isolation techniques, and diverse functions in cancer progression. *Front. Immunol.* 9, 738. doi:10.3389/fimmu.2018.00738
- Xia, Y., Hu, X., Di, K., Liu, C., Tan, T., Lin, Y., et al. (2020). Combined detection of exosome concentration and tumor markers in gastric cancer. *J. Biomed. Nanotechnol.* 16, 252–258. doi:10.1166/jbn.2020.2887
- Xie, H., Di, K., Huang, R., Khan, A., Xia, Y., Xu, H., et al. (2020). Extracellular vesicles based electrochemical biosensors for detection of cancer cells: A review. *Chin. Chem. Lett.* 31, 1737–1745. doi:10.1016/j.ccl.2020.02.049
- Yang, H., Liang, W., He, N., Deng, Y., and Li, Z. (2015). Chemiluminescent labels released from long spacer arm-functionalized magnetic particles: a novel strategy for ultrasensitive and highly selective detection of pathogen infections. *ACS Appl. Mat. Interfaces* 7, 774–781. doi:10.1021/am507203s
- Yang, Q., Cheng, L., Hu, L., Lou, D., Zhang, T., Li, J., et al. (2020). An integrative microfluidic device for isolation and ultrasensitive detection of lung cancer-specific exosomes from patient urine. *Biosens. Bioelectron.* X, 163, 112290. doi:10.1016/j.bios.2020.112290
- Yu, W., Hurley, J., Roberts, D., Chakraborty, S., Enderle, D., Noerholm, M., et al. (2021). Exosome-based liquid biopsies in cancer: opportunities and challenges. *Ann. Oncol.* 32, 466–477. doi:10.1016/j.annonc.2021.01.074
- Zhang, Z., Tang, C., Zhao, L., Xu, L., Zhou, W., Dong, Z., et al. (2019). Aptamer-based fluorescence polarization assay for separation-free exosome quantification. *Nanoscale* 11, 10106–10113. doi:10.1039/c9nr01589b
- Zhang, P., Zhou, X., He, M., Shang, Y., Tetlow, A. L., Godwin, A. K., et al. (2019). Ultrasensitive detection of circulating exosomes with a 3D-nanopatterned microfluidic chip. *Nat. Biomed. Eng.* 3, 438–451. doi:10.1038/s41551-019-0356-9
- Zhao, Y., Fang, X. X., Zhao, Y. X., Zhang, J., Yu, H., Chen, F., et al. (2022). A microfluidic surface-enhanced Raman scattering (SERS) sensor for microRNA in extracellular vesicles with nucleic acid-tyramine cascade amplification. *Chin. Chem. Lett.* 33, 2101–2104. doi:10.1016/j.ccl.2021.08.047
- Zhu, F. J., Ji, Y. H., Lu, Y., Li, L., Bai, X., Liu, X., et al. (2022). Microfluidics-based technologies for the analysis of extracellular vesicles at the single-cell level and single-vesicle level. *Chin. Chem. Lett.* 33, 2893–2900. doi:10.1016/j.ccl.2021.09.058